Monthly Notices of the ROYAL ASTRONOMICAL SOCIETY

MNRAS **466,** L98–L102 (2017) doi:10.1093/mnrasl/slw244
Advance Access publication 2016 December 5

A strongly truncated inner accretion disc in the Rapid Burster

J. van den Eijnden,[1,2⋆] T. Bagnoli,[2,3] N. Degenaar,[1,2] A. M. Lohfink,[1] M. L. Parker,[1] J. J. M in 't Zand[3] and A. C. Fabian[1]

[1] *Institute of Astronomy, University of Cambridge, Madingley Road, Cambridge CB3 0HA, UK*
[2] *Anton Pannekoek Institute for Astronomy, University of Amsterdam, Science Park 904, NL-1098 XH Amsterdam, the Netherlands*
[3] *SRON – Netherlands Institute for Space Research, Sorbonnelaan 2, NL-3584 CA Utrecht, the Netherlands*

Accepted 2016 December 1. Received 2016 November 28; in original form 2016 November 3

ABSTRACT

The neutron star (NS) low-mass X-ray binary (LMXB) the Rapid Burster (RB; MXB 1730-335) uniquely shows both Type I and Type II X-ray bursts. The origin of the latter is ill-understood but has been linked to magnetospheric gating of the accretion flow. We present a spectral analysis of simultaneous *Swift*, *NuSTAR* and *XMM–Newton* observations of the RB during its 2015 outburst. Although a broad Fe K line has been observed before, the high quality of our observations allows us to model this line using relativistic reflection models for the first time. We find that the disc is strongly truncated at $41.8^{+6.7}_{-5.3}$ gravitational radii (∼87 km), which supports magnetospheric Type II burst models and strongly disfavours models involving instabilities at the innermost stable circular orbit. Assuming that the RB magnetic field indeed truncates the disc, we find $B = (6.2 \pm 1.5) \times 10^8$ G, larger than typically inferred for NS LMXBs. In addition, we find a low inclination ($i = 29^{\circ} \pm 2^{\circ}$). Finally, we comment on the origin of the Comptonized and thermal components in the RB spectrum.

Key words: accretion, accretion discs – stars: neutron – X-rays: binaries – X-rays: individual: MXB 1730-335.

1 INTRODUCTION

The Rapid Burster [MXB 1730-335 (hereafter RB), Lewin et al. 1976 is a peculiar neutron star (NS) low-mass X-ray binary (LMXB) located at a distance of 7.9 kpc in the globular cluster Liller-1 (Valenti, Ferraro & Origlia 2010). NS LMXBs often show X-ray bursts, either due to thermonuclear burning of accreted material on the NS surface (Type I) or due to a sudden release of gravitational energy (Type II). The RB is one of the only two NSs showing Type II X-ray bursts and the only source showing both types. It typically displays only Type I bursts at high persistent luminosities, and both burst types at lower ones (Bagnoli et al. 2013). Various models for the poorly understood Type II bursts have been proposed, including magnetospheric gating of the accretion flow (Spruit & Taam 1993; see Bagnoli et al. 2015 for a recent overview of models), in which a strong NS magnetic field truncates the accretion disc outside the innermost stable circular orbit (ISCO; sixR_g for a non-spinning NS, where $R_g = GM/c^2$ is the gravitational radius). Measuring the inner disc radius can thus provide a direct test of such magnetospheric models for the RB.

Constraining the accretion geometry in LMXB is possible by modelling the reflection spectrum (Fabian et al. 1989): hard X-ray emission reflected off the accretion disc, which prominently contains a gravitationally and dynamically broadened Fe K line at ∼6.5 keV. Using this approach, Degenaar et al. (2014) find an inner disc radius of $R_{in} = 85.0 \pm 10.9 R_g$ in the Bursting Pulsar [GRO J1744−28 (hereafter BP), Kouveliotou et al. 1996], the other source showing Type II bursts. This truncation is much larger than typically observed in NS LMXBs (6–15R_g, see e.g. Cackett et al. 2010 for a sample study). Hence, the question arises whether a similar truncation is present in the RB. In this Letter, we present an analysis of new, simultaneous observations of the RB using *Swift*, *NuSTAR* and *XMM–Newton*, aimed at constraining the inner disc radius.

2 OBSERVATIONS

2.1 *Swift*

As RB outbursts are relatively predictable, a *Swift* (Gehrels et al. 2004) X-ray Telescope (XRT) monitoring campaign was carried out in Window Timing (WT) mode to detect the start of the outburst. An outburst was detected on 2015 October 3 and triggered, simultaneous *NuSTAR* and *XMM–Newton* observations were performed on October 6. A single ∼500 s *Swift* observation (obsID 00031360129) coincided with the *NuSTAR* and *XMM–Newton* observations. For this observation, we use XSELECT v2.4d to extract an XRT spectrum from a 70.8 arcsec radius aperture. We create an arf using XRTMKARF, take the rmf (v15) from the CALDB, and rebin the spectrum to ensure a minimum of 20 counts per bin using

⋆ E-mail: a.j.vandeneijnden@uva.nl

GRPPHA. As *Swift*-WT observations of bright, absorbed sources tend to show residuals below ∼1 keV,[1] we fit the *Swift* spectrum only in the 1–10 keV range.

2.2 *NuSTAR*

NuSTAR (Harrison et al. 2013) observed the RB between 2015 October 6 12:11:08 and 7 15:11:08 (obsID 90101009002), amounting to ∼46 ks on-target exposure time for both focal plane modules (FMP) A and B. This full exposure consists of ∼40 ks non-burst and ∼6 ks burst exposure (see Section 3 for the determination of burst intervals). We apply the standard routines NUPIPELINE and NUPRODUCTS to extract source and background spectra for the non-burst and burst intervals separately. We extract source spectra from a 120-arcsec-radius circular aperture. As the source dominates its chip, we extract background spectra from a same-sized region on the opposite chip. However, we find no significant differences with background spectra extracted from either the two remaining chips or a smaller background region on the source chip. The source spectrum dominates above the background up to ∼30 keV, so we fit the *NuSTAR* spectra in the range of 3–30 keV.

2.3 *XMM–Newton*

XMM–Newton(Jansen et al. 2001) observed the RB between 2015 October 6 19:23:44 and October 7 06:12:20 (obsID 0770580601) with the EPIC-pn in timing mode and MOS1/2 turned off, resulting in ∼18 ks on-target exposure (of which ∼3 ks burst exposure). We process the observation data files using *XMM–Newton* SAS v15. For the RGS detector, we apply RGSPROC to extract event lists for non-burst and burst intervals separately. After assuring that no background flaring is present, we combine spectra of the same order from the two RGS detectors using RGSCOMBINE and rebin to a minimum of 20 counts per bin. The extracted spectra show discrepancies between the two orders, and between the RGS and XRT spectra, below 1 and above 2 keV. Hence, we only consider the range of 1–2 keV for the RGS spectra. In this work, we do not search for narrow features in the RGS spectra.

The EPIC-pn spectrum (extracted using EPPROC and EPCHAIN with quality flag =0, pattern ≤4) shows cross-calibration issues with the *Swift* and *NuSTAR* spectra: the continuum slope above ∼5 keV differs significantly between the spectra. Similar issues in timing mode observations of black hole binaries in the hard state have been reported recently (see e.g. Ingram et al. 2017). Given the consistency between the *Swift* and *NuSTAR* spectra, we decide to exclude the EPIC-pn spectra.

3 SPECTRAL FITTING

The *NuSTAR* and *XMM–Newton* light curves contain no Type I bursts and in total 56 Type II bursts, an example of which is shown in Fig. 1. Measuring the time of the minima in the characteristic dips before and after each burst, we manually define the non-burst and burst intervals used in the extraction of the spectra. Per instrument, we extract a single burst spectrum combining all Type II bursts. This burst spectrum contains ∼47 per cent (FMPA, FMPB) and ∼39 per cent (RGS) of the total counts in the observation. The

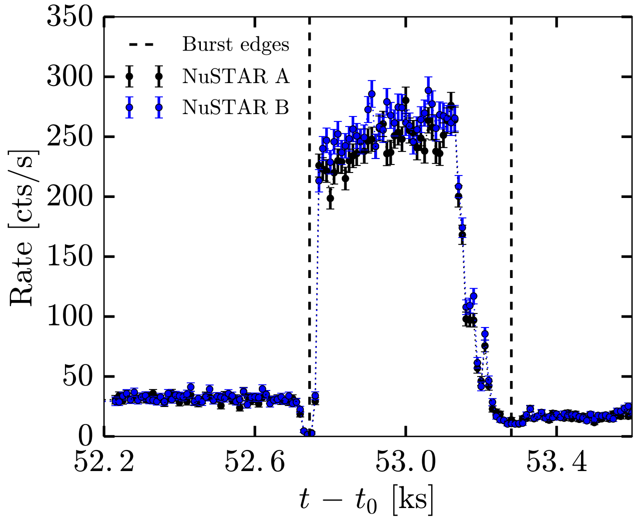

Figure 1. Representative example of a Type II burst in the *NuSTAR* observation. The characteristic dips, visible before and after the burst, form the border between the non-burst and burst GTIs. The start time of the observation is t_0.

Swift observation coincides fully with a non-burst interval. We initially focus on the non-burst spectrum, and discuss on the burst spectrum at the end of Section 3.2.

We use XSPEC v12.9.0 (Arnaud 1996) for the spectral fitting and assume solar abundances from Wilms, Allen & McCray (2000) and cross-sections from Verner et al. (1996). We model interstellar absorption using TBABS and include a free constant between all spectra fixed to 1 for the FMPA spectrum). All quoted uncertainties are at 1σ.

3.1 Phenomenological modelling

Falanga et al. (2004) fit an *Integral* spectrum (3–100 keV) of the RB with a model consisting of a power law, a blackbody and a Gaussian Fe K line. We adopt a similar approach, but replace the power law with the physically motivated Comptonization model COMPTT (Titarchuk 1994). This model yields a reasonable fit with $\chi^2_\nu = 1.32$ (3265/2477), and the inclusion of the blackbody component is required at high significance ($\Delta\chi^2/\Delta$d.o.f $= 277/2$). For the Gaussian component, we measure $E_{\rm G} = 6.50 \pm 0.02$ keV and $\sigma_{\rm G} = 0.86 \pm 0.03$ keV, consistent with Falanga et al. (2004). However, this phenomenological modelling does not provide us with a statistically satisfactory fit, and a Gaussian does not adequately describe the feature around ∼6.5 keV. Hence, we turn to relativistic reflection modelling of the non-burst spectrum.

3.2 Relativistic reflection modelling

For our reflection fits, we replace the Gaussian line with the model REFLIONX (Ross & Fabian 2005). We apply an adapted version of this model, which was calculated with a COMPTT illuminating spectrum instead of a power law,[2] as COMPTT is dominant in the phenomenological fit at all energies. To include relativistic effects, we convolve REFLIONX with RELCONV (Dauser et al. 2010). We link

[1] See http://www.swift.ac.uk/analysis/xrt/digest_cal.php#abs.

[2] http://www-xray.ast.cam.ac.uk/~mlparker/reflionx_models/reflionx_comptt_hightau.mod

Table 1. Model parameters for the tbabs(comptt +gauss+soft component+relconv*reflionx)-models. All quoted uncertainties are at 1σ. We fix $q = 3$ and $a = 0.0$.

Component	Parameters (unit)	BB-model	disc-model
TBABS	$N_{\rm H}$ (10^{22} cm^{-2})	3.17 ± 0.03	3.64 ± 0.03
COMPTT	T_0 (keV)	1.54 ± 0.01	1.56 ± 0.01
	$kT_{\rm e}$ (keV)	7.19 ± 0.08	7.12 ± 0.08
	τ	$1.01^{+0.30}_{-0.11}$	$1.00^{+0.20}_{-0.11}$
	Norm (10^{-2})	1.07 ± 0.03	1.10 ± 0.03
GAUSS	Norm (10^{-4})	1.66 ± 0.35	1.83 ± 0.34
DISCBB	$kT_{\rm disc}$ (keV)	–	$0.73^{+0.02}_{-0.01}$
	Norm	–	138 ± 15
BBODYRAD	$kT_{\rm BB}$ (keV)	0.55 ± 0.01	–
	Norm	450 ± 40	–
RELCONV	i ($^{\rm o}$)	29 ± 2	32 ± 2
	$R_{\rm in}$ ($R_{\rm g}$)	$41.8^{+6.7}_{-5.3}$	$49.5^{+9.2}_{-7.0}$
REFLIONX	ξ	470^{+61}_{-14}	460 ± 10
	$A_{\rm Fe}$	$0.71^{+0.08}_{-0.06}$	0.77 ± 0.06
	Norm	$10.8^{+0.4}_{-0.9}$	$10.4^{+0.3}_{-0.5}$

the input soft photon temperature T_0, electron temperature $kT_{\rm e}$ and optical depth τ between COMPTT and REFLIONX. We fix the dimensionless spin parameter $a = 0.0$, as for NSs this value ranges from 0.0 to 0.3 and has little effect on the surrounding metric (see e.g. Miller, Lamb & Cook 1998). Indeed, setting $a = 0.3$ does not yield significant changes in either the model parameters or the quality of the fit. Furthermore, we assume an unbroken emissivity profile with a fixed slope of $q = 3$, as the slope is not contrained by the data. This value is consistent with both theoretical expectations (Wilkins & Fabian 2012) and results from a sample study in NS LMXBs by Cackett et al. (2010). The disc ionization, parametrized as $\xi \equiv 4\pi F/n$, where F is the illuminating flux and n the hydrogen number density, is left variable. In addition, we leave the inclination i, inner disc radius $R_{\rm in}$ and iron abundance $A_{\rm Fe}$ free to vary.

We attempt two possibilities for a soft component: DISCBB and BBODYRAD (the complete models are hereafter referred to as the disc- and BB-model, respectively). Furthermore, inspection of the residuals around the Fe K line suggests the presence of an additional narrow emission line around 6.4 keV. Hence, we also include a narrow Gaussian ($\sigma = 10^{-3}$) fixed at this energy of 6.4 keV.

The disc-model yields a good fit, with $\chi^2_\nu = 1.13$ (2789/2472) for a temperature $kT_{\rm disc} = 0.73^{+0.02}_{-0.01}$ keV. The BB-model results in the best fit, with $\chi^2_\nu = 1.10$ (2727.8/2472) for a temperature $kT_{\rm bb} = 0.55 \pm 0.01$ keV. All other parameters are listed in Table 1. Most interestingly, the reflection component implies a large disc truncation in both models: $R_{\rm in} = 41.8^{+6.7}_{-5.3} R_{\rm g}$ for the BB-model and $R_{\rm in} = 49.5^{+9.2}_{-7.0} R_{\rm g}$ for the disc-model, both significantly larger than commonly observed in NS LMXBs (e.g. Cackett et al. 2010). Both models also yield a consistent, low inclination estimate of $\sim 30^{\rm o}$ and an intermediate disc ionization of $\xi \sim 470$. The latter is consistent with the typical range observed in both black hole and NS LMXBs [log (ξ) $\sim$ 2–3]. The BB-model yields an unabsorped flux between 1–30 keV of 1.47×10^{-9} erg cm^{-2} s^{-1}, corresponding to a luminosity of 1.23×10^{37} erg s^{-1} (at a distance of 7.9 kpc) and an Eddington ratio of $\sim$3.2 per cent assuming the emperical Eddington luminosity determined by Kuulkers et al. (2003).

Fig. 2 shows the spectra and the best-fitting relativistic reflection + blackbody model. Fig. 3 shows the confidence contours for the inner disc radius and the inclination. Both parameters are clearly

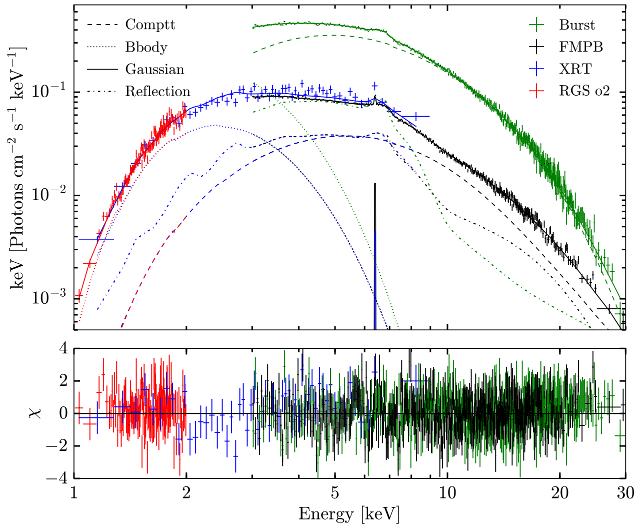

Figure 2. The *NuSTAR* (FMPB), *XMM–Newton* RGS (order 2) and *Swift* unfolded spectra with the best-fitting TBABS (COMPTT + BBODYRAD + RELCONV*REFLIONX + GAUSS) model. For clarity, we show only a single spectrum per telescope. For comparison, we also show the unfolded FMPA burst spectrum in green. The spectra have been rebinned for visual purposes in XSPEC using SETPLOT REBIN. Note that small deviations appear visible in the *Swift*-spectrum between 2 and 3 keV.

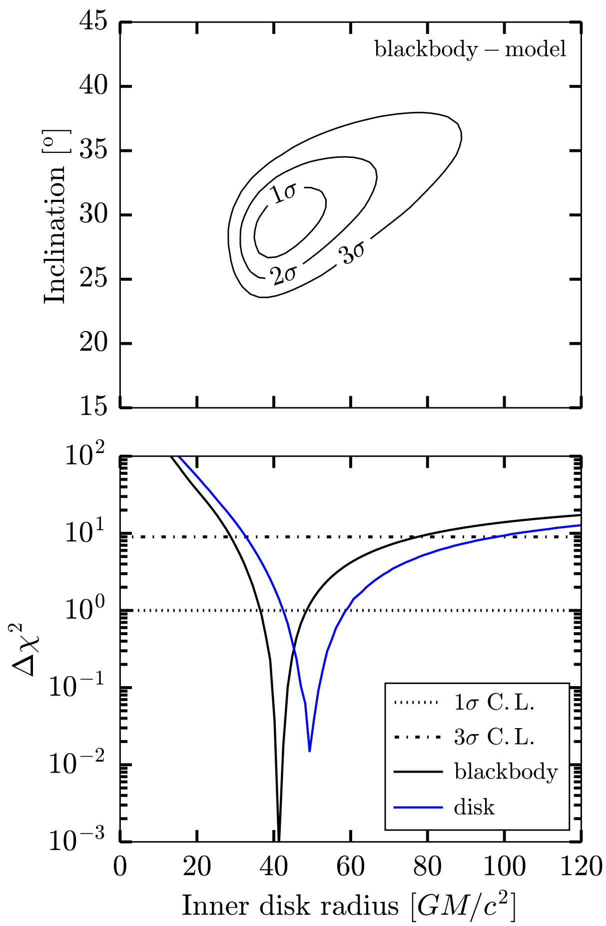

Figure 3. Top panel: 2D confidence contour for the inclination and inner disc radius or the BB-model. Bottom panel: confidence plot of the inner disc radius for the blackbody and disc-models.

well constrained by the data, and the inner disc radius is inconsistent with the ISCO (i.e. $6R_g$) at $\gtrsim 14.1\sigma$ ($\Delta\chi^2 \gtrsim 200$) for either model.

The emission line at 6.4 keV is significant at $\sim 5\sigma$ for both models, given the uncertainty in the normalization. This line, consistent with neutral iron, is also seen in the BP (Degenaar et al. 2014), although it is more generally observed in high-mass X-ray binaries (Torrejón et al. 2010). Letting its energy vary does not provide a significant improvement of the fit (f-test probability $p > 0.01$ for both models). The residuals in Fig. 2 also suggest the presence of an absorption line around 6.9 keV. However, the addition of a Gaussian absorption line is not statistically significant.

Fitting the BB-model to the RGS and *NuSTAR* burst spectra (see Fig. 2) yields a poorly constrained inclination and R_{in}. Thus, we instead fit the burst and non-burst spectra simultaneously, tying the column density and inclination. This results in a good fit ($\chi^2_\nu = 1.11$ (4744.1/4272)) as now the non-burst data constrains the inclination at $i = 22^\circ \pm 1^\circ$. We measure $R_{in} = 40.1^{+3.3}_{-2.8} R_g$, consistent with the non-burst value. R_{in} is inconsistent with the ISCO at $\gtrsim 8\sigma$. The burst spectrum is significantly softer, yielding a lower electron temperature of $kT_e = 2.42 \pm 0.03$ keV. Finally, the Comptonized component is much stronger relative to the reflection spectrum during burst intervals.

4 DISCUSSION

We present a spectral analysis of simultaneous *NuSTAR*, *XMM–Newton* and *Swift* observations of the RB, aimed at constraining its accretion geometry and the origin of its peculiar Type II burst behaviour. The non-burst spectrum is well described by a combination of the Comptonization model COMPTT, relativistic reflection of this Comptonized emission (RELCONV*REFLIONX), a soft (disc)blackbody and a narrow emission line at 6.4 keV. From the reflection spectrum, we measure a large inner disc truncation radius ($\sim$40–$50R_g$) and a low inclination ($\sim$30°). Here, we will discuss the nature of the disc truncation, the implications for Type II burst models, and the origin of the spectral components.

4.1 The nature of the truncated disc

NS LMXBs show a wide range of inferred inner disc radii, which can roughly be divided into three categories: most sources show small inner disc radii of 6–$15R_g$ (12 LMXBs, see Cackett et al. 2010; Degenaar et al. 2015; Di Salvo et al. 2015; Ludlam et al. 2016; Sleator et al. 2016). Secondly, five NS LMXBs, mostly (intermittent) X-ray pulsars, show a slightly larger inner radius of roughly 15–$30R_g$ (Iaria et al. 2016; Miller et al. 2011; Papitto et al. 2013; Pintore et al. 2016; King et al. 2016). Finally, two sources show significantly larger truncation radii: Degenaar et al. (2017) infer $R_{in} \gtrsim 100R_g$ for IGR J17062-6143, an LMXB persistently accreting a low rates ($L_X \approx 4 \times 10^{35}$ erg s^{-1}). Although various possible explanations exist for a truncated disc at such low L_X, truncation by the magnetosphere would imply a large NS magnetic field ($\gtrsim 4 \times 10^8$ G). Furthermore, Degenaar et al. (2014) measure $R_{in} = 85.0 \pm 10.9R_g$ in the BP. Our result places the RB in this third category of large disc truncations. As only the RB and the BP show Type II bursts, the presence of a large disc truncation in both forms an interesting constraint of Type II burst models.

Models for Type II bursts can be divided into different general categories (see Bagnoli et al. 2015, for a review): instabilities in the accretion flow, general-relativistic instabilities close to the ISCO, and interactions between the accretion disc and the NS magnetic field. As only two LMXBs show Type II bursts, it is difficult to distinguish between these options. However, the first type of model is unable to account for the uniqueness of the RB and the BP: such instabilities should be observed more generally among NS LMXBs. The second category is strongly disfavoured by our inner disc radius measurement, as it requires the disc to extend up to the ISCO.

The most prominent model of accretion instabilities driven by a disc-magnetic field interaction is a so-called *trapped disc* (Spruit & Taam 1993; D'Angelo & Spruit 2010). At the magnetospheric radius R_m, the disc is truncated by the magnetic field (see e.g. Pringle & Rees 1972). If the NS spin frequency exceeds the Keplerian rotation frequency of the disc at this radius R_m, the magnetic field prevents accretion, confining infalling material in the disc (Sunyaev & Shakura 1977; Spruit & Taam 1993), or, alternatively, resulting in outflows (Illarionov & Sunyaev 1975). As matter piles up, the magnetospheric radius moves inwards, until the Keplerian frequency exceeds the NS spin, matter swiftly accretes and R_m moves out again. This trapped-disc model is consistent with our measurement of a large truncation radius in the RB, and the similar result for the BP by Degenaar et al. (2014). Additionally, in this scenario a change in R_{in} might be expected during bursts. However, the size of such a change in inner radius is unknown; given the relatively large uncertainties on R_{in} (5–$10R_g$), we might simply be unable to detect such changes significantly in our observations.

Assuming that the disc is truncated by the magnetic field, we can estimate the magnetic field of the RB using Equation (1) in Cackett et al. (2009). We estimate a bolometric flux of $F_{bol} = (2.25 \pm 0.2) \times 10^{-9}$ erg cm^{-2} s^{-1} by extrapolating the best fit over the 0.1–100 keV range. Using geometrical and efficiency parameters from Cackett et al. (2009), we find $B = (6.2 \pm 1.5) \times 10^8 (M/1.4\,M_\odot)^2 (R/10\,\mathrm{km})^{-3}$ G. This estimate is higher than generally observed for NS LMXBs (Mukherjee et al. 2015). A similarly high magnetic field as in the RB is present in the 11-Hz pulsar IGR J17480-2446 in Terzan 5 (Miller et al. 2011). This strengthens the proposed link between these two sources (Bagnoli et al. 2013) and indicates that the RB, like IGR J17480-2446, could be young, mildly recycled LMXB (Patruno et al. 2012). However, a spin measurement for the RB remains necessary to confirm this scenario.

4.2 Completing the geometrical picture

Falanga et al. (2004) fit the continuum in a 3–100 keV *Integral* spectrum with a combination of a power law and a blackbody. The blackbody parameters ($kT_{BB} \sim 2.2$ keV, $R_{BB} \sim 1.4$ km) suggest that this continuum might originate from a hotspot on the NS surface, as expected if the magnetic field truncates the disc, or a boundery layer. Instead, we fit the continuum above 3 keV using a COMPTT-component, which might thus arise from such a hotspot or boundary layer (instead of, for example, a corona). In the trapped-disc model, such an origin could also explain the large increase in the COMPTT-flux during bursts.

As we also have high-quality data below 3 keV, we detect an additional soft blackbody component unseen by *Integral*. Its temperature is consistent with the expectation for the NS surface at the inferred accretion rate (Zampieri et al. 1995), although the implied radius of 16.7 km is larger than expected for NSs ($\sim$10 km). However, Zampieri et al. (1995) also show that the surface spectrum might slightly deviate from a perfect blackbody. These deviations in the surface spectrum might thus explain why the BBODYRAD model infers a larger radius than expected. If the soft component indeed corresponds to the NS surface, it completes a self-consistent geometrical description of the RB spectrum with a large truncation radius and a hotspot on the NS surface.

ACKNOWLEDGEMENTS

We thank the referee for comments on this Letter. JvdE and ND are supported by a Vidi grant from the Netherlands Organization for Scientific Research (NWO) awarded to ND. ND also acknowledges support via a Marie Curie fellowship (FP-PEOPLE-2013-IEF-627148) from the European Commission. ACF, AL and MP are supported by Advanced Grant Feedback 340442 from the European Research Counsil (ERC). TB acknowledges support from NewCompStar (COST Action MP1304). JvdE and TB acknowledge the hospitality of the Institute of Astronomy in Cambridge, where this research was carried out. We are grateful to Fiona Harrison, Norbert Schartel, Neil Gehrels and the observation planners for making these Director's Discretionary Time observations possible.

REFERENCES

Arnaud K. A., 1996, in Jacoby G. H., Barnes J., eds, ASP Conf. Ser. Vol. 101, Astronomical Data Analysis Software and Systems V. Astron. Soc. Pac., San Francisco, p. 17
Bagnoli T., in't Zand J. J. M., Galloway D. K., Watts A. L., 2013, MNRAS, 431, 1947
Bagnoli T., in't Zand J. J. M., D'Angelo C. R., Galloway D. K., 2015, MNRAS, 449, 268
Cackett E. M., Altamirano D., Patruno A., Miller J. M., Reynolds M., Linares M., Wijnands R., 2009, ApJ, 694, L21
Cackett E. M. et al., 2010, ApJ, 720, 205
D'Angelo C. R., Spruit H. C., 2010, MNRAS, 406, 1208
Dauser T., Wilms J., Reynolds C. S., Brenneman L. W., 2010, MNRAS, 409, 1534
Degenaar N., Miller J. M., Harrison F. A., Kennea J. A., Kouveliotou C., Younes G., 2014, ApJ, 796, L9
Degenaar N., Miller J. M., Chakrabarty D., Harrison F. A., Kara E., Fabian A. C., 2015, MNRAS, 451, L85
Degenaar N., Pinto C., Miller J. M., Wijnands R., Altamirano D., Paerels F., Fabian A. C., Chakrabarty D., 2017, MNRAS, 464, 398
Di Salvo T. et al., 2015, MNRAS, 449, 2794
Fabian A. C., Rees M. J., Stella L., White N. E., 1989, MNRAS, 238, 729
Falanga M., Farinelli R., Goldoni P., Frontera F., Goldwurm A., Stella L., 2004, A&A, 426, 979
Gehrels N. et al., 2004, ApJ, 611, 1005
Harrison F. A. et al., 2013, ApJ, 770, 103
Iaria R. et al., 2016, A&A, 596, A21
Illarionov A. F., Sunyaev R. A., 1975, A&A, 39, 185
Ingram A., Van der Klis M., Middleton M., Altamirano D., Uttley P., 2017, MNRAS, 464, 2979
Jansen F. et al., 2001, A&A, 365, L1
King A. L. et al., 2016, ApJ, 819, L29
Kouveliotou C., van Paradijs J., Fishman G. J., Briggs M. S., Kommers J., Harmon B. A., Meegan C. A., Lewin W. H. G., 1996, Nature, 379, 799
Kuulkers E., den Hartog P. R., in't Zand J. J. M., Verbunt F. W. M., Harris W. E., Cocchi M., 2003, A&A, 399, 663
Lewin W. H. G. et al., 1976, ApJ, 207, L95
Ludlam R. M. et al., 2016, ApJ, 824, 37
Miller M. C., Lamb F. K., Cook G. B., 1998, ApJ, 509, 793
Miller J. M., Maitra D., Cackett E. M., Bhattacharyya S., Strohmayer T. E., 2011, ApJ, 731, L7
Mukherjee D., Bult P., van der Klis M., Bhattacharya D., 2015, MNRAS, 452, 3994
Papitto A. et al., 2013, MNRAS, 429, 3411
Patruno A., Alpar M. A., van der Klis M., van den Heuvel E. P. J., 2012, ApJ, 752, 33
Pintore F. et al., 2016, MNRAS, 457, 2988
Pringle J. E., Rees M. J., 1972, A&A, 21, 1
Ross R. R., Fabian A. C., 2005, MNRAS, 358, 211
Sleator C. C. et al., 2016, ApJ, 827, 134
Spruit H. C., Taam R. E., 1993, ApJ, 402, 593
Sunyaev R. A., Shakura N. I., 1977, Sov. Astron. Lett., 3, 138
Titarchuk L., 1994, ApJ, 434, 570
Torrejón J. M., Schulz N. S., Nowak M. A., Kallman T. R., 2010, ApJ, 715, 947
Valenti E., Ferraro F. R., Origlia L., 2010, MNRAS, 402, 1729
Verner D. A., Ferland G. J., Korista K. T., Yakovlev D. G., 1996, ApJ, 465, 487
Wilkins D. R., Fabian A. C., 2012, MNRAS, 424, 1284
Wilms J., Allen A., McCray R., 2000, ApJ, 542, 914
Zampieri L., Turolla R., Zane S., Treves A., 1995, ApJ, 439, 849

This paper has been typeset from a TEX/LATEX file prepared by the author.